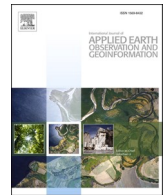




Contents lists available at ScienceDirect

International Journal of Applied Earth Observation and Geoinformation

journal homepage: www.elsevier.com/locate/jag



Uncertainty analysis for forest height inversion using L / P band PolInSAR datasets and RVoG model over kryclan forest site

Han Zhao^a, Tingwei Zhang^a, Yongjie Ji^b, Wangfei Zhang^{a,*}

^a Forestry College, Southwest Forestry University, Kunming 650224, China

^b School of Geography and Ecotourism, Southwest Forestry University, Kunming 650224, China



ARTICLE INFO

Keywords:

Uncertainty

PolInSAR

RVoG

Forest height

Canopy type

Forest density

ABSTRACT

Forest height, as a measure of the quantity and quality of forest resources, plays a significant role in the study of the ecological functions performed by forests. Although the polarimetric synthetic aperture radar interferometry (PolInSAR) technique has evolved as a potent method for forest height inversion, uncertainties still exist in the process of estimating forest height, and the uncertainties in predicted forest height directly lead into the uncertainty of terrestrial carbon stock calculation results. In this study, we took the Random Volume over Ground (RVoG) model as likelihood function and constructed a hierarchical Bayesian framework to calculate and reduce the uncertainty of forest height inversion using L / P band PolInSAR airborne data via RVoG model. Uncertainties resulted from five canopy types and three forest densities were analyzed, respectively. The results showed that among the five different canopy types, L band has the highest prediction accuracy in pure coniferous canopy with Acc. = 0.90. The uncertainty is extremely low for pure forest, with the ratio of uncertainty values of 0.09 for L band and 0.15 for the P band in pure coniferous canopy, and uncertainty values of 0.16 for L band and 0.11 for P band in pure broadleaf canopy, respectively. Furthermore, when the forest density is between 300 and 600 stems/ha, the ratio of uncertainties for the L band is 0.27, whereas the P band is 0.24. As forest density increases, the uncertainty in forest height estimates decreases for both bands. The changes in canopy types and forest density affect forest height estimation uncertainties obviously, the effects are different at each frequency. The forest height inversion accuracy of the L band in pure coniferous canopy surpasses that in other canopy types, with the lowest uncertainty. P band performed well in broadleaf canopy forest height inversion. The inversion uncertainties at both frequencies decrease with increase of forest densities.

1. Introduction

Forest height is an essential forest vertical structural characteristic that is closely associated with carbon stock coming from forest above-ground biomass (AGB) (Pang et al., 2022). Accurate forest height distribution knowledge plays a key role in monitoring forest development, disturbance, and degradation. Obtaining accurate forest height information plays a significant role for forest management, carbon circulation and worldwide warming researches (Xu et al., 2022; Kugler et al., 2015).

Longer-wavelength synthetic aperture radar (SAR) like L and P band have great forest penetration capabilities, excellent inversion accuracy and then have great potential for forest height inversion, especially when combined with polarimetric synthetic aperture radar interferometry (PolInSAR) techniques. (Cloude and Papathanassiou, 2003; Liao

et al., 2020; Wu et al., 2022). Given the implementation of European Space Agency's (ESA) P band BIOMASS SAR and L-band interferometric SAR satellite program of China, mapping forest height or AGB across the globe with measurements using L / P band PolInSAR datasets become available and necessary. This increased availability of data will further facilitate their extensive use in forest height inversion (Xing et al., 2023). Indeed, although PolInSAR methodology has been determined to be an efficient solution for forest height retrieval, there are still various uncertainties associated with the estimated results using this technique. These uncertainties in forest height estimated results can significantly affect the accuracy and quality of terrestrial carbon stock simulations and forecasts (Riel et al., 2018; Lang et al., 2022). Therefore, it is urgent to explore the uncertainties of the estimated forest height results using PolInSAR methodology.

The Random Volume over Ground (RVoG) model has become a

* Corresponding author.

E-mail address: zhangwfw@swfu.edu.cn (W. Zhang).

commonly employed physical vegetation scattering model for forest height retrieval utilizing the PolInSAR technique in the last twenty years (Romero-Puig et al., 2022). Since the original RVoG model was assumed on the scattering mechanisms of L band in forests, it was addressed better inversion performance in low frequencies such as L or P band (Papathanassiou and Cloude, 2001). Meanwhile, the uncertainties of the estimated forest height are as important as height estimates themselves in many scientific applications. For instance, these uncertainties in forest height estimated results can significantly affect the accuracy and quality of terrestrial carbon stock simulations and forecasts (Riel et al., 2018; Lang et al., 2022). Uncertainties of the estimated forest height via RVoG model depend on the input observations, the estimation method used, and the appropriateness of the model to relate the observations to model parameters (Riel et al., 2018; Zhang et al., 2023a; 2023b). Moreover, uncertainties associated with imaging, processing, and scene parameters also contribute to uncertainties on PolInSAR-estimated forest height. For instance, effects resulted from effective number of looks, terrain correction, range bandwidth on calculating the observed coherences to estimate the forest height (Riel et al., 2018). Uncertainties resulted from the inversion methods selected for forest height via RVoG like polarimetric phase center height estimation method (PPC), complex coherence phase center differencing algorithm (CCPCD), coherence amplitude inversion method (CAI), and hybrid inversion method using both phase and coherence information (Zhang et al., 2022). Furthermore, the RVoG model might not be suitable for forests with an orientated structure or when temporal decorrelation existing, which could lead to overestimated or underestimated canopy heights (López-Martínez and Alonso-González, 2013). Estimating Forest height via RVoG model is a multistage procedure, the procedure includes stages like inputting observation coherence values, coherence optimization, ground phase calculation and forest height. Errors accumulated at each stage will be propagated to each consecutive stage. The uncertainties resulted from each stage are nonlinear, for example the errors during coherence optimization and ambiguity resulted in ground phase estimation. Therefore, linearizing the uncertainties resulted from each stage and using propagation of uncertainties to pass it from one stage to next stage may mischaracterize the final uncertainties (Riel et al., 2018).

Uncertainty analyses for RVoG model estimated forest heights typically involve two approaches: direct validation with external precise measurement data, such as LiDAR or ground-based forest height surveys, and probabilistic modeling techniques like Monte Carlo simulations and Bayesian methods (Simard and Denbina, 2018; Zhang et al., 2023b). For the uncertainty validated by an external dataset, the results are often influenced by the quality of externally datasets and also their co-registration quality with existing inversion results. Some researchers have used probabilistic models for uncertainty analysis. Kugler et al. (2015) employed a Monte Carlo approach to perform repetitive and stochastic inversions of the RVoG model on PolInSAR data, which in turn determines the uncertainty of the inversion results. However, this method only considers the uncertainty in the observed data and does not adequately take into account modelling errors or uncertainty resulted from the prior knowledge. Simard and Denbina (2018) added a prior knowledge of each input parameter of the model based on the study of Kugler et al (2015). The external LiDAR working as a prior knowledge to fix the extinction coefficients or temporal decorrelation significantly improves the accuracy of the forest height inversion and reduces the uncertainty of the inversion results (Simard and Denbina, 2018). Riel et al. (2018) used a Bayesian model with the RVoG model working as likelihood function to simultaneously analyze the uncertainty resulting from the model input parameters and the uncertainty arising from the model theoretical assumptions, observations, etc., and the results of the study demonstrated the feasibility of the Bayesian framework in the study on the uncertainty of the estimated forest heights using PolInSAR technique.

In the data observation process, factors such as the effective number of looks, range bandwidth, and signal-to-noise ratio affect the coherence

and phase quality, thereby introducing uncertainties (Kugler et al., 2015; Riel et al., 2018). These can typically be corrected by the data acquisition agency, such as using information provided by them to eliminate the impact of signal-to-noise ratio (Zhao et al., 2022; Krieger, et al., 2007). In the data processing stage, critical steps such as co-registration quality, phase noise, and temporal decorrelation compensation also directly influence the uncertainty of the forest height inversion results. Co-registration can typically be handled by the data providers (Zhao et al., 2022; Tebaldini et al., 2023), ensuring co-registration quality. Phase noise can be suppressed through filtering methods. Furthermore, the impact of temporal decorrelation can usually be mitigated by selecting observations with zero temporal baselines or through different modeling and compensation methods (Hajnsek et al., 2009; Lee et al., 2013; Papathanassiou and Cloude, 2003; Simard and Denbina, 2018). Our previous studies explored the uncertainties resulted from selection of forest height inversion methods (Zhang et al., 2022) and the forest structure (Zhang et al., 2023a) using the simulated PolInSAR images. Although several researchers have conducted extensive studies on most of the uncertainty factors in the PolInSAR forest height inversion process, however, the related field still exist research gaps. For example, the effects of the wavelength operated in SAR datasets on the uncertainties of the inversion results, forest structures like canopy types composed of trees with only coniferous trees, only broadleaf trees and mixture of both coniferous and broadleaf trees, and forest densities on uncertainties of the inversion results are not fully addressed yet, especially using Bayesian framework.

To address these research gaps, in this study, L and P band PolInSAR data acquired during the BioSAR campaign were utilized to retrieve forest height using the RVoG model. And simultaneously, the RVoG model was incorporated into a hierarchical Bayesian framework to investigate uncertainties arising from variations in forest canopy structure and density.

2. Material and methods

2.1. Test site

The location of the test site is in the watershed of the Krycklan River ($64^{\circ}24'N$, $19^{\circ}79'E$, Fig. 1), north of Sweden. It is covered 6,700 ha of boreal forestry. The land features a hilly topography with moderate slopes and the elevation ranges from 20 to 400 m (Neumann et al., 2012). Coniferous and broadleaf forests are primary forest types with the dominated tree species of *Betula spp*, *Pinus sylvestris*, and *Picea abies*. The mean forest height at the measured test site is around 18 m, with an upper limit of roughly 30 m (Soja et al., 2013).

2.2. Data acquisition and data processing

The SAR datasets employed in this paper were collected by DLR with an experimental airborne SAR (E-SAR) system and known as BioSAR campaign. L and P band PolInSAR images were acquired in October 2008 (Hajnsek et al., 2009; Li et al., 2015). Specific information of the configuration of the imaging parameters is given in Table 1. The incidence angles of the acquired PolInSAR datasets range from about 25° to 60° , with 12 m for azimuthal resolution and 8.33 m for range resolution (Hajnsek et al., 2009).

The LiDAR data was collected simultaneously at the study site. The laser scanning of Krycklan catchment as part of the BIOSAR 2008 campaign was performed on the 5th and 6th of August 2008 with the TopEye system S/N 425 mounted on a helicopter. It was conducted at a flight altitude of 500 m above ground level for main strips and 250 m above ground level for cross strips. Approximately 70 km^2 was covered with an average point density of approximately 5 points per square meter in the main strips and 15 points per square meter in the cross strips. Additional details on the laser scanning can be found in Hajnsek (2009). The acquired point cloud datasets were used to derive canopy

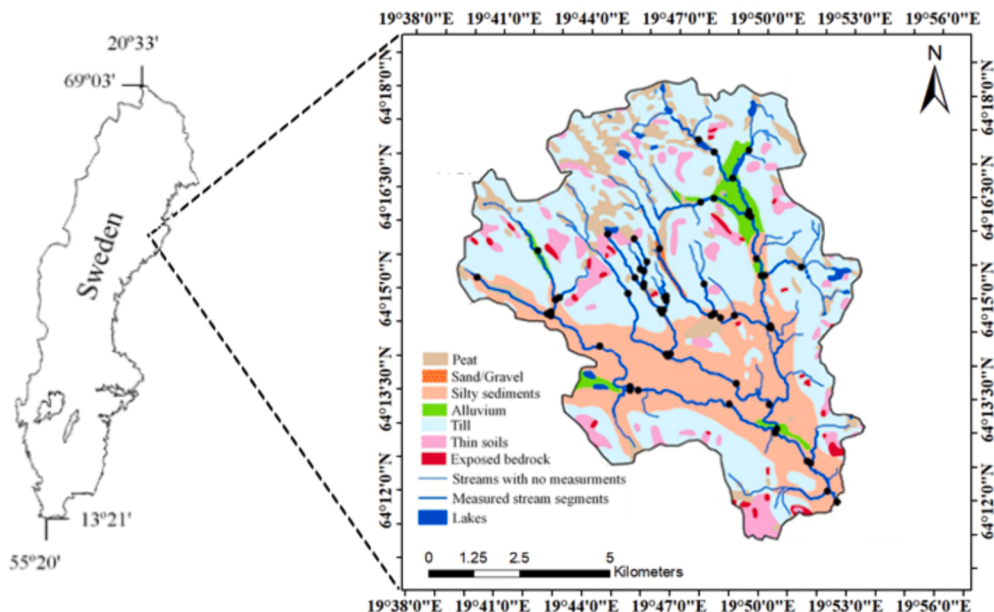


Fig. 1. The location of the study area.

Table 1
Airborne PolInSAR data parameters.

Image ID	Band	Baseline/m	Mean of k_z ¹ rad/m	Angles of incidence	Centre frequency	Acquisition date
0201	L	Master	Master	25–55°	1300 MHz	2008.10.15
0209	L	24	0.48	25–55°	1300 MHz	2008.10.15
0103	P	Master	Master	25–55°	350 MHz	2008.10.14
0107	P	16	0.06	25–55°	350 MHz	2008.10.14

¹ k_z : Vertical Wavenumber.

height model (CHM) which is used in this study for validation and related forest height extraction. The pixel size of the derived CHM product is 0.5 m (Fig. 2). The forest height values in the CHM range from 0 to 39 m.

With the BioSAR campaign, a total of 31 forest stands were surveyed for extensive field measurements with diverse shapes and sizes from 1.5 to 22 ha. Each stand includes approximately 10 circle plots with radius of 10 m. In each plot, trees with diameter at breast height (DBH) larger than 4 cm were measured and recorded. A total of 12,390 single trees were measured in this field campaign, in which tree species, forest height, and plot density were recorded. Most of the collected stand samples were mixed with *Betula spp.*, *Pinus sylvestris*, and *Picea abies*. To study the uncertainty resulting from the different canopy types and forest densities during the forest height estimation using PolInSAR data, in this research we selected seven forest stands (71 plots) from the 31 forest stands to analyze the uncertainty. Five canopy types including pure coniferous canopy, pure broadleaf canopy, mixed coniferous canopy, mixed broadleaf canopy, and mixed coniferous and broadleaf canopy (Fig. 3, Table 2) were classified and used for uncertainty analysis of the effect from change of canopy types. Forest density was categorized into 3 groups like 300–600 stems/ha, 600–1200 stems/ha, and 1200–1800 stems/ha in the study area and to consider uncertainty resulted from changes of forest density. All of the information of the seven forest stands was collected on 13 October 2008.

ESA has performed master and slave image co-registration when provided BioSAR data to the user, then the preprocessing of the BioSAR PolInSAR data in this paper includes multi-look, flat earth phase estimation and remove, interferometric image generation, and interferometric multi-coherence estimation. The number of multi-look for the

SAR data in this paper is 3 for azimuth and 1 for range, the complex coherence computation window size is 11; and the pre-processing of the PolInSAR datasets are conducted in ENVI IDL and PolSARpro 4.2.

2.3. Methods

In this research, RVoG models were first used for forest height inversion via L and P band PolInSAR datasets. Then the RVoG model was worked as a likelihood function and introduced to a hierarchical Bayesian framework to calculate the related posterior probability distribution function and then used for uncertainty analysis and reduction in forest height inversion. The key parameters σ (extinction coefficient) and γ_t (temporal decorrelation) in RVoG models were decided according to the relationship analysis between RVoG model parameters and uncertainties using Bayesian framework in former research (Riel et al., 2018; Simard and Denbina, 2018).

2.3.1. RVoG model

RVoG model establishes a relationship between forest height and polarimetric interference complex coherence (Cloude and Papathanassiou, 1998; Zhang et al., 2017). Forest scene in RVoG model is assumed and divided into two layers. The vegetation layer is modeled as a volume layer with thickness of h_v , in which randomly oriented particles are distributed uniformly. This layer is modeled by an exponential structure function characterized by a mean wave extinction coefficient σ . The ground layer is presumed sufficiently lossy, and the surface is rough to an extent that only surface-volume scattering need be considered. The observed interferometric coherences can be related to the forest height through equation (1):

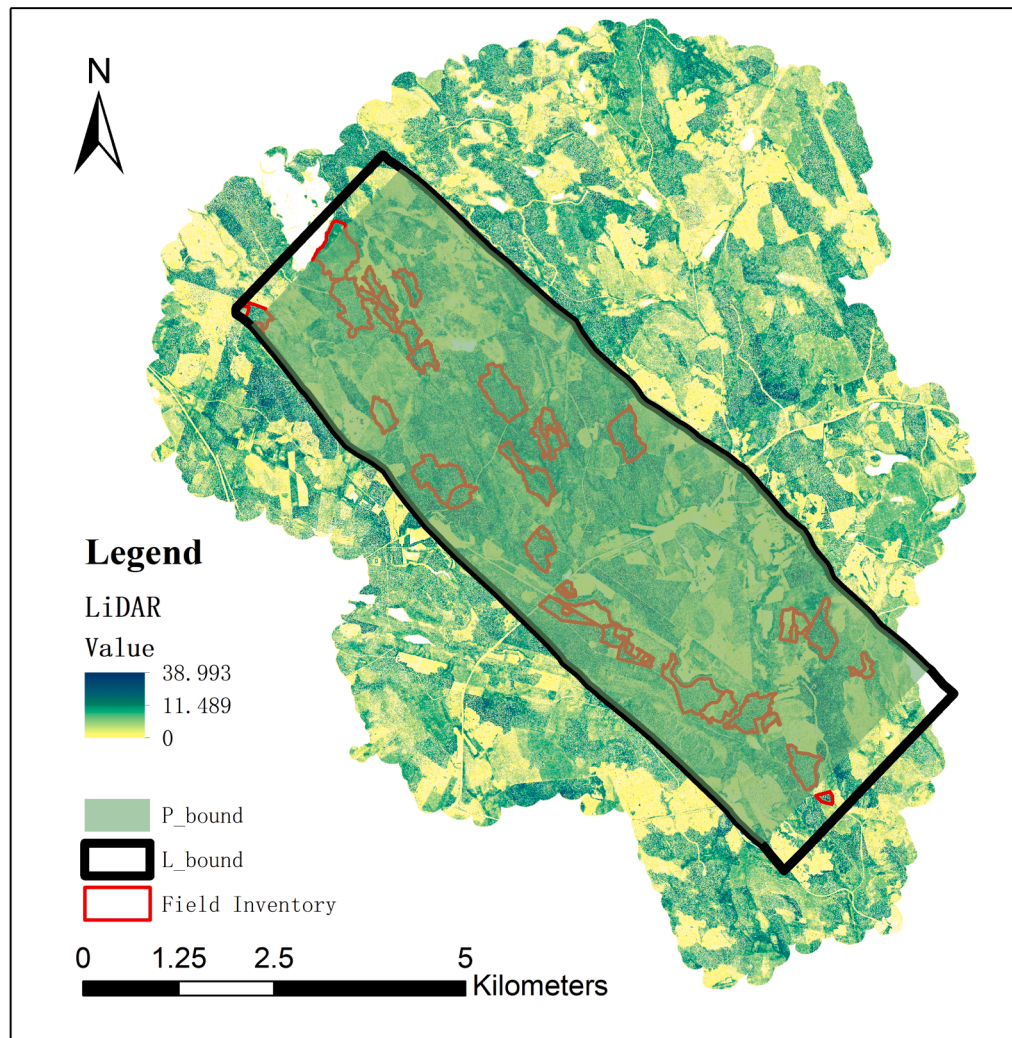


Fig. 2. Forest height distribution map extracted from the LiDAR data.

$$\gamma = R(\mathbf{m}) + \epsilon \quad (1)$$

where γ is the vector of observed complex coherence for each polarimetric channel, $R(\bullet)$ presents the RVoG model, \mathbf{m} represents the vector of model variables, and ϵ corresponds to the error array with an assumption of Gaussian distribution of mean = 0 and variance = $\sigma^2 \gamma$. Equation (2) is the constructed RVoG model:

$$R(\mathbf{m}) = \exp(i\phi_0) \frac{\gamma_v + \mu}{1 + \mu} \quad (2)$$

where ϕ_0 is ground phase center, μ is effective ground-to-volume scattering ratio, and γ_v is forest volume complex coherence, it is a function of the forest height h_v and the extinction coefficient σ , its exponential function is like equation (3):

$$\gamma_v = \frac{p_1(\exp(p_2 h_v) - 1)}{p_2(\exp(p_1 h_v) - 1)} \begin{cases} p_1 = \frac{2\sigma}{\cos\theta} \\ p_2 = \frac{2\sigma}{\cos\theta} + ik_z \end{cases} \quad (3)$$

where k_z is effective vertical wavenumber, θ is local incidence angle, k_z and θ are decided by the imaging geometry of the SAR platform.

In (3), since k_z and θ are known, ϕ_0 is decided by the phase of surface-dominated polarization vector which can be found through the distribution of different polarimetric channels (scattering mechanisms) on the complex plane (Tabb et al., 2002). A set of determined h_v and σ values

can be acquired by a unique value of γ_v (Cloude and Papathanassiou, 2003).

If the temporal decorrelation is not considered in RVoG model, it leads to erroneous and/or biased coherence and then leads to an overestimation of forest heights (Reigber and Moreira, 2000;

Lavalle and Hensley, 2015). Previous studies introduced several ways to compensate temporal decorrelation (TD) (Cloude and Papathanassiou, 2003; Simard and Denbina, 2018; Lavalle and Khun, 2014; Lavalle et al., 2012). However, most of them introduced new assumptions and add new parameters, which will result in the non-unique solution of the model and the complexity of the solution process. In these cases, the models can only be solved by introducing external reference data to reduce the number of unknowns, or by adding independent observations. In order to reduce the additional uncertainty introduced from the assumption from TD, the volume temporal decorrelation (VTD) model was incorporated in RVoG model and used here to compensate for TD effect. In VTD model, it is assumed that TD only results in the change of coherence amplitude but no effect on phase shift, and then RVoG VTD model can be described as equation (4) by adding a TD of γ_t which is polarization dependent in RVoG model (Papathanassiou and Cloude, 2003). In this study, γ_t can be decided based on the LiDAR derived forest height values at the test site.

$$R(\mathbf{m}) = \exp(i\phi_0) \frac{\gamma_t \gamma_v + \mu}{1 + \mu} \quad (4)$$

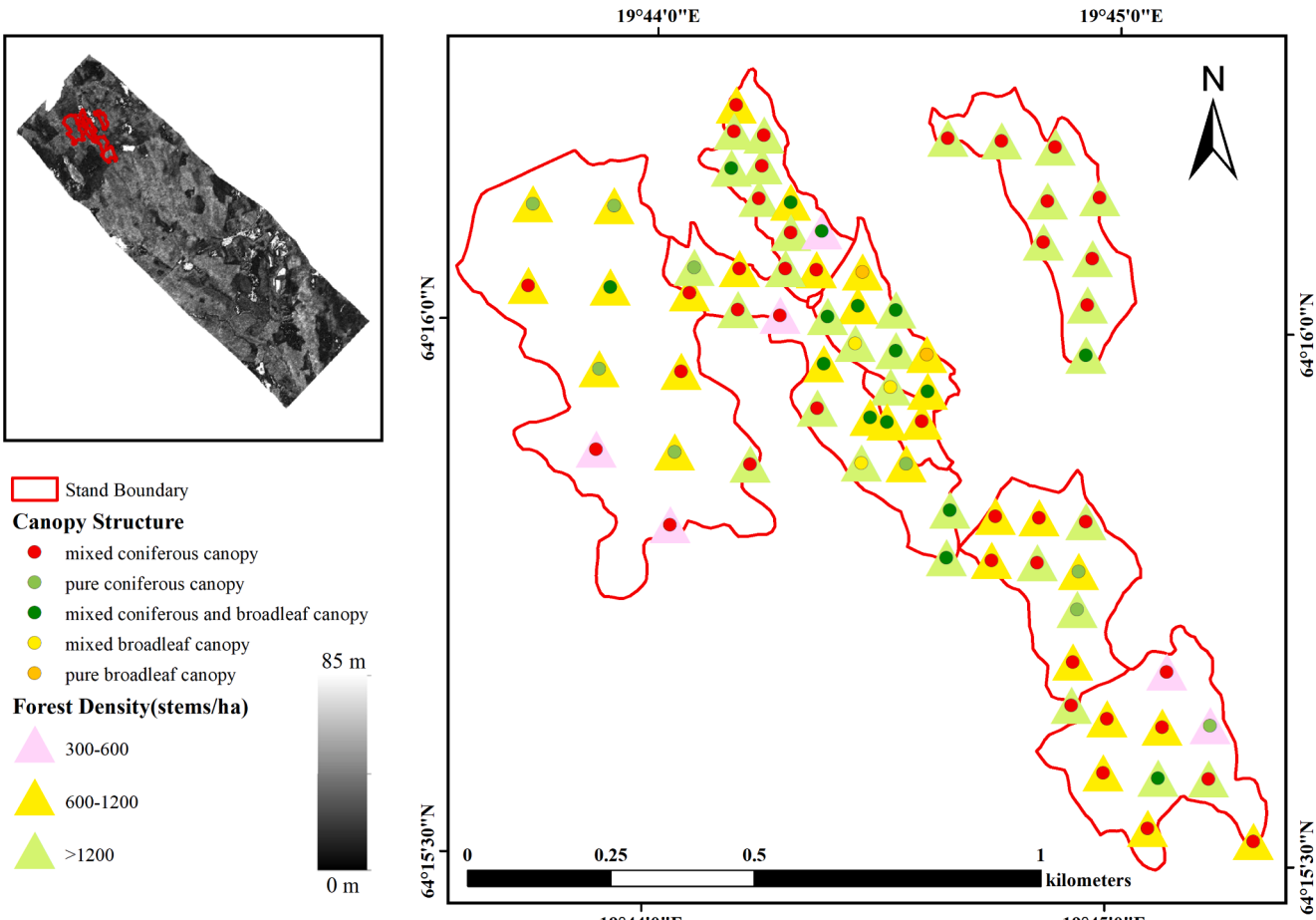


Fig. 3. The Distribution of the selected stands and the sample plots with different canopy types (mixed coniferous canopy, pure coniferous canopy, mixed coniferous and broadleaf canopy, mixed broadleaf canopy, mixed broadleaf canopy, and pure broadleaf canopy) and forest densities (300–600 stems/ha, 600–1200 stems/ha, and greater than 1200 stems/ha).

Table 2
Detail information of the selected 7 field collected sample plots.

Stand ID	Average age/year	Average forest height /m	Average forest density (stems /ha)
1493	77.45	13.07	1451.49
1517	61.22	14.08	752.37
1812	57.05	13.12	1126.82
1892	107.46	16.94	873.58
15,096	124.87	15.73	1294.46
18,147	90.67	14.26	1837.1
18,278	86.88	13.87	1380.98

2.3.2. Hierarchical Bayesian framework for RVoG models

The basic theory and framework of original Bayesian method and multi-parameter Bayesian method had been introduced in our previous study (Zhang et al., 2023a). According to the basic Bayesian framework, a posterior probability distribution $p(\mathbf{m}|\gamma, R(\mathbf{m}))$ was constructed by equation (5). The prior probability $p(\mathbf{m})$ is the probability function of the model parameter of \mathbf{m} from RVoG with observed data γ and a scattering model of $R(\mathbf{m})$. With $p(\mathbf{m}|\gamma, R(\mathbf{m}))$ and adequate samples, the uncertainties resulted from each parameter in \mathbf{m} is decided and then optimized model parameters with lower uncertainty were chose and used for forest height inversion.

$$p(\mathbf{m}|\gamma, R(\mathbf{m})) \propto p(\gamma|\mathbf{m}, R(\mathbf{m}), \sigma_\gamma) p(\mathbf{m}) \quad (5)$$

To better quantify the errors resulted from observed data and model

procedure, equation (5) was extended as equation (6) to incorporate the knowledge of σ_γ by a hierarchical Bayesian model.

$$p(\mathbf{m}, \sigma_\gamma | \gamma, R(\mathbf{m})) \propto p(\gamma | \mathbf{m}, R(\mathbf{m}), \sigma_\gamma) p(\mathbf{m}) p(\sigma_\gamma) \quad (6)$$

Where $p(\mathbf{m}, \sigma_\gamma | \gamma, R(\mathbf{m}))$ is the Bayesian posterior probability distribution function of the inversed forest height of the RVoG model, which is the joint distribution of error parameter σ_γ and model parameter \mathbf{m} , $p(\gamma | \mathbf{m}, R(\mathbf{m}), \sigma_\gamma)$ is the likelihood function representing the probability of the observed data input to the model and a particular collection of model parameters. The hyperprior $p(\sigma_\gamma)$ is the prior distribution of σ_γ (Riel et al., 2018).

Hierarchical Bayes allows to obtain the uncertainty in the error between predicted coherence and observation coherence by adding a hyperparameter, and assimilates multiple sources of uncertainty into a single stochastic parameter for a specific pixel. Through applied (6) in forest height estimated by RVoG model, a more realistic uncertainty metrics on forest height were obtained (Riel et al., 2018).

2.3.3. Uncertainty analysis and reduce by hierarchical Bayesian framework

In this study, the utilization of the Bayesian framework with PolInSAR data is implemented for each pixel in the estimated RVoG height maps as follows:

- (1) TD compensation. In order to eliminate the effect of TD and greatly reduce the uncertainty contribution resulted from TD, we first use a priori knowledge to fix TD. The TD values for each pixel

- were calculated by introduce the LiDAR true forest height value into the RVoG VTD model, then use the calculated TD value as a fix value to the RVoG VTD model (Simard and Denbina, 2018);
- (2) Priori distribution function setting for equation (6). A Gaussian prior distribution was used for $p(m)$. The height obtained by the RVoG with fixed TD works as the mean value and ± 10 meters as the standard deviation for prior distribution function of Gaussian according to previous studies (Riel et al., 2018). A uniform distribution as the prior distribution for the extinction coefficient σ , and the variation range of σ is from 0 to 1.5 dB/m according to the penetration capability of L- or P-band (Riel et al., 2018). An inverse gamma hyperprior was set for $p(\sigma_\gamma)$ and a likelihood function of Gaussian was set for $p(\gamma|m, R(m), \sigma_\gamma)$.
 - (3) Bayesian posterior distribution calculation and applied for uncertainty decrease. Posterior distribution $p(m, \sigma_\gamma | \gamma, R(m))$ for the RVoG-estimated forest height was calculated according to equation (6) and step (2). Since the posterior distribution does not have a fixed function format, the Markov chain Monte Carlo (Metropolis-Hastings) is used here to extract approximate samples from the posterior distribution. During the sampling procedure, find_MAP function provided by PyMC3 was used to obtain the maximum a posteriori estimation points of the parameters. The number of sampling chain here is 2, and 50,000 samples are obtained based on each sampling chain. The first 10,000 samples were eliminated to increase the stability of the sampling chain. The sampling procedure was repeated twice to reduce the random errors and the best sampling results in the two sampling chains were chosen for next qualification of uncertainties analysis.

2.3.4. Quantification of uncertainties

The ratio of uncertainty is used in this study to describe the uncertainty of estimated forest height. It is the degree of ambiguity about the measured value due to the presence of measurement error and can be used to estimate measurement reproducibility. If the indirectly measured parameter (forest height) is a function of the directly measured observations (input parameters of the RVoG model), the ratio of the uncertainty of the indirect measurement can be expressed as the synthesized uncertainty of the uncertainty resulted from each directly measured measurement (Xiao, 1985; Li, 2003). In this paper, according to the technical specification of JJF1059.1-2012 “Measurement Uncertainty Assessment and Representation”, the ratio of the uncertainty is assessed in class A using Bessel’s method, the involved equations include (7)-(14) (Ni, 2014).

$$\varepsilon_i = x_i - X_i \quad (7)$$

$$\delta_i = \frac{x_i - X_i}{x_i} \quad (8)$$

$$Acc. = 1 - \delta_i \quad (9)$$

$$|\varepsilon_i| = |x_i - X_i| \quad (10)$$

$$\bar{X} = \frac{1}{n} \sum_{i=1}^n X_i \quad (11)$$

$$S^2(X_i) = \frac{1}{n-1} \sum_{i=1}^n (X_i - \bar{X})^2 \quad (12)$$

$$U(X_i) = S(X_i) = \sqrt{\frac{\sum_{i=1}^n (X_i - \bar{X})^2}{n-1}} \quad (13)$$

$$U(\bar{X}) = S(\bar{X}) = \frac{S(X_i)}{\sqrt{n}} \quad (14)$$

where ε_i is the prediction error, x_i is the true value, X_i is the sample of forest height inversion results from SAR data obtained by simulation under the reproducibility condition (Ni, 2014), δ_i is the relative error, Acc. is the prediction accuracy, accuracy characterizes the deviation between true values and predicted values; $|\varepsilon_i|$ is the absolute error, n is sample numbers, \bar{X} is the arithmetic mean value for observations, $S^2(X_i)$ and $U(X_i)$ are the experimental variance and the experimental standard deviation, respectively, $U(\bar{X})$ is the ratio of uncertainty of the inversion results, which represents the confidence level in the inverted value due to the existence of errors in the inversion results. It also characterizes the reproducibility of the experiment and the standard deviation of the distribution of results from a large number of repeated trials.

3. Results and discussion

3.1. Forest height acquired from PolInSAR dataset and Bayesian framework

In this study, forest height was first estimated and mapped through RVoG. 150 samples were randomly selected for the estimating of forest heights and their uncertainty analysis. The 150 samples were selected through fishnet tools in ArcGIS software in each canopy type or forest density. The related mean LiDAR value was considered as the true value, and prediction accuracy along with the ratio of uncertainty were calculated. Fig. 4 showed the mapping results from forest height inversed by RVoG model. The estimated forest height values in Fig. 4 are used for mean and standard deviation of assumed priori Gaussian distribution. To avoid anomalous values in the estimated results especially in regions of low coherence, forest heights at regions with $|\gamma| < 0.3$ in the coherence map were masked and removed from the height map. The left values in the forest height map were used for sampling in ArcGIS. A fishnet with 0.5 m interval was created in ArcGIS and for forest height sampling and the selected samples were applied in the latter Bayesian framework construction and analysis.

The constructed Gaussian distribution working as the priori distribution of forest height, then the posterior distribution was calculated according steps introduced in section 2.3.3. Although the calculated posterior distribution $p(m, \sigma_\gamma | \gamma, R(m))$ for the estimated forest height is not a closed-form solution, we plot it (Fig. 5(1)) according the samples in Fig. 5(b). Fig. 5(b) shows an example of sampling points track in a pixel using the constructed posterior distribution and Metropolis-Hastings method. The sampling time of each pixel of this sampling chain is about 18 s. The study from Riel et al. (2018) used same steps confirmed the uncertainties resulted from RVoG model parameters like σ , γ_t , k_z , observed coherences, ground phase estimation. Our previous study (Zhang, et al., 2023b) also demonstrated the effectiveness using sampling method of Metropolis-Hastings to quantify the uncertainties of the estimated results (Riel et al., 2018; Zhang, et al., 2023b).

Probabilistic framework based on Bayesian theorem was demonstrated effective for estimating lower bound variance of Cramer-Rao on forest height estimated from RVoG (Roueff et al., 2011). Similar forest height estimation procedure and uncertainty analysis were applied in a simulated L-band PolInSAR datasets with simulated forest scenes (Zhang, et al., 2023a).

3.2. Qualitative analysis of the uncertainties of the estimated results

With the calculated posterior distribution for h_y and introduced sampling method in section 4.1, forest heights were produced utilizing a Bayesian framework at L-band (Fig. 6(a)) and P-band (Fig. 6(b)), the difference between forest heights and CHM values derived from LiDAR at L-band (Fig. 6(c)) and P-band (Fig. 6(d)), and estimation uncertainty

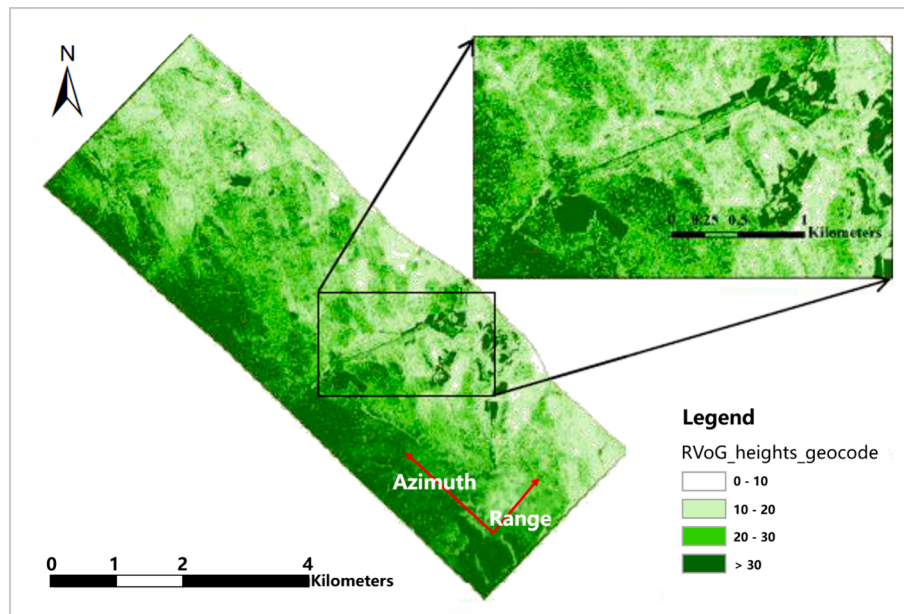


Fig. 4. Forest height map the inversed results using RVoG model and PolInSAR data (P-band shows here as an example).

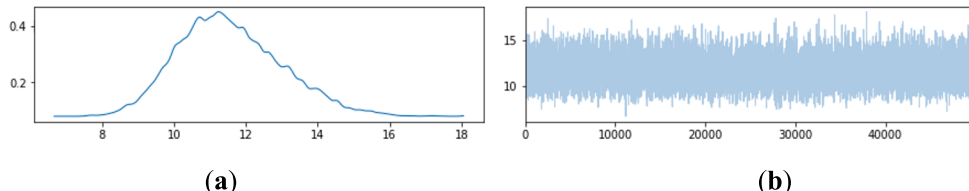


Fig. 5. Posterior distribution of sampling height. (a) A posterior distribution of forest height, the horizontal label is forest height values, and the vertical label is the frequency of the related forest height values; (b) An example of sampling points track in a pixel using the constructed posterior distribution and Metropolis-Hastings method. The horizontal label is the number of the sampled points, the vertical label is forest height.

(standard deviation) of forest height at L-band (Fig. 6(e)) and P-band (Fig. 6(f)) were computed and mapped.

In Fig. 6, we calculated forest height for each pixel through averaging value of samples acquired by the related sampling chain. The absolute errors of the estimated results are the disparities between the calculated forest heights and LiDAR derived values at the same location of every pixel. The uncertainty is described by the standard deviation of sampling. Fig. 6 demonstrated that regions with larger heights in LiDAR product show bigger uncertainties and larger deviations. In addition, comparing Fig. 3 with Fig. 6, we found that larger absolute errors seem to located near mixed forests. The phenomenon is similar both at L / P band. In fact, higher forest heights are derived from lower coherence which may ultimately affects the accurate value of the inferred volumetric coherence (Kugler et al., 2015). When compared the results from L and P band, we found the estimated forest heights acquired from L band show higher uncertainty than that acquired at P band. The reason needs to be further explored. At both bands, high uncertainty is obvious at sparse area, it is correspondent with the RVoG model assumption as well (Cloude and Papathanassiou, 2003; Zhang, et al., 2023b).

To further explore the relationships between uncertainties and the forest height, Fig. 7 reported the scatterplots between height uncertainty and related height. At L band (Fig. 7a), the uncertainties increase with the improving of forest height, while at P band, an inverse gamma distribution appears in the red box of Fig. 7b. Many sample points with lower heights also show large uncertainties, which may be due to the greater penetrability of the P band with its longer wavelengths that results in a complex scattering of the P band in forest canopy. Since the large ground-to-volume scattering ratio at P band than L band and also

the smaller extinction coefficients, they may result in the unsuitable model assumption of RVoG at P band.

Nonetheless, most of the uncertainty values lie in the range of 0–3 m for L band estimated heights between 10 and 20 m, while most of them at P band has the similar uncertainty interval but the estimated heights are between 5 to 15 m. However, all of them indicates uncertainties of 10 %–20 %, which is widely recognized in PolInSAR community in past researches (Riel et al., 2018; Lavalle and Hensley, 2015; Hajnsek et al., 2009; Cloude, 2009).

3.3. Quantitative analysis of the uncertainties of the estimated results

In order to further analyze the impacts of canopy types and forest density on the forest height estimated results, we categorized the inversion results according to five different canopy types. Meanwhile, different forest densities including 300–600 stems/ha, 600–1200 stems/ha and greater than 1200 stems/ha were grouped and applied for further qualitative analysis of the uncertainty of the estimated results. 150 samples were randomly selected from the estimated forest heights of each forest stand. Mean LiDAR value works as true values, prediction accuracy and the ratio of uncertainty were calculated and the statistical information is summarized in Table 3 (statistical uncertainty resulted from changes of canopy type) and Table 4 (statistical uncertainty resulted from changes of forest density).

Canopy types show obvious effects on forest height inversion uncertainties. L band showed better performance in coniferous canopy with lower values for uncertainty and the ratio while P band showed better performance in broadleaf canopy. The best performance of L band

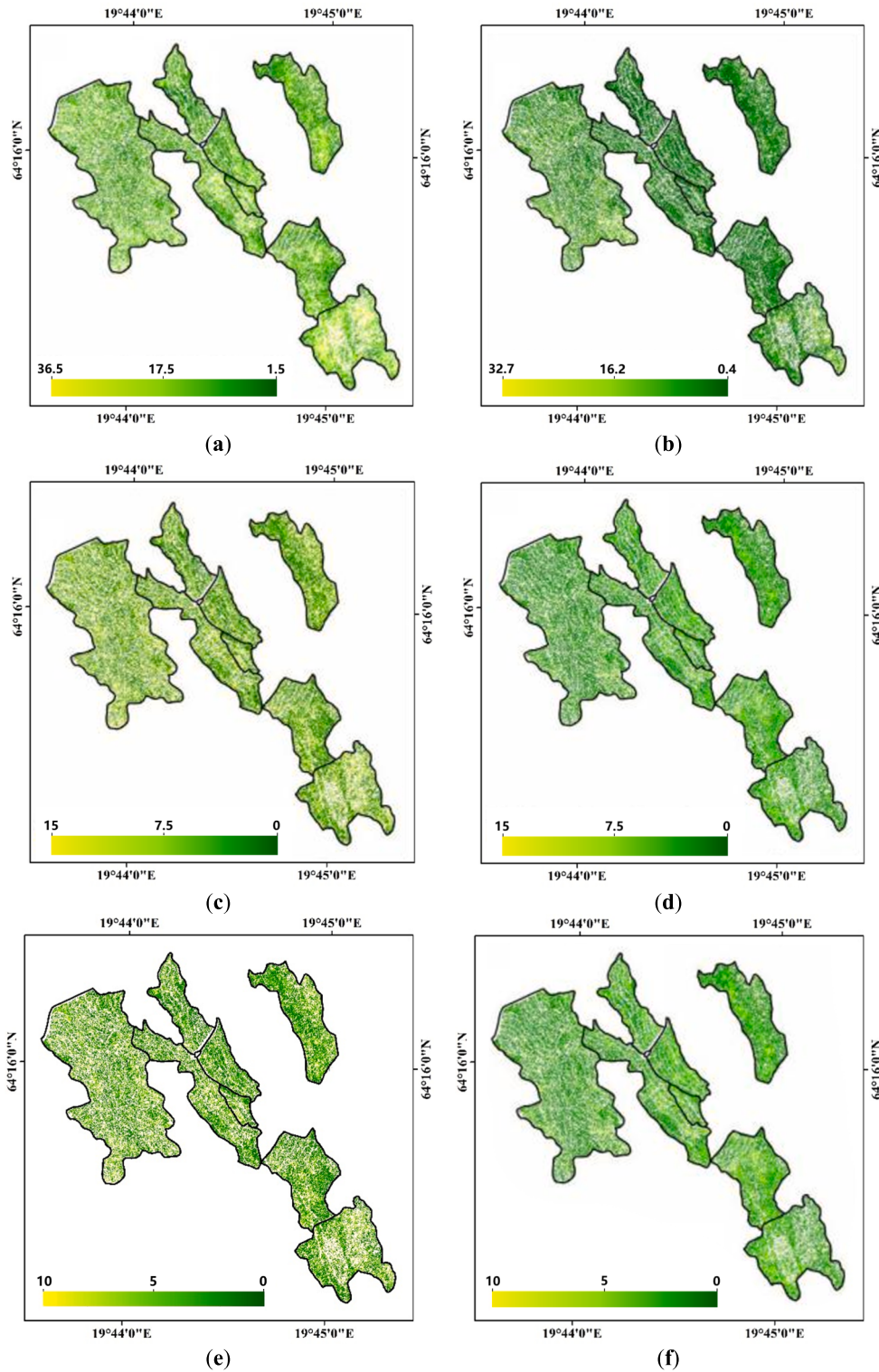


Fig. 6. Forest height estimation results, absolute error and stand deviation. (a) sampled forest height at L band; (b) sampled forest height at P band; (c) absolute error at L band; (d) absolute error at P band and LiDAR heights; (e) standard deviation at L band; (f) standard deviation at P band.

is in pure coniferous canopy with $U(\bar{X}) = 0.09$ and $Acc. = 0.90$. The lowest estimation accuracy using L band was acquired in mixed coniferous and broadleaf canopy with $Acc. = 0.55$. The highest ratio of uncertainty for estimated results using L band observations was acquired in mixed broadleaf canopy with $U(\bar{X}) = 0.25$. The best performance of P band is in pure broadleaf canopy with $U(\bar{X}) = 0.13$ and $Acc. = 0.78$. Next is mixed broadleaf canopy with a $Acc.$ of 0.77 and then is mixed

coniferous and broadleaf canopy with $Acc. = 0.75$. The ratios of the uncertainty in the three canopy types at P band is 0.09, 0.13 and 0.26, respectively. Both frequencies performed better in pure forest while worse in mixed forest. However, estimated forest height using P band in mixed canopy type showed less difference with its performance in pure canopy type than that using L band. The results revealed the potential of L band in pure coniferous canopy and the potential of P band in both

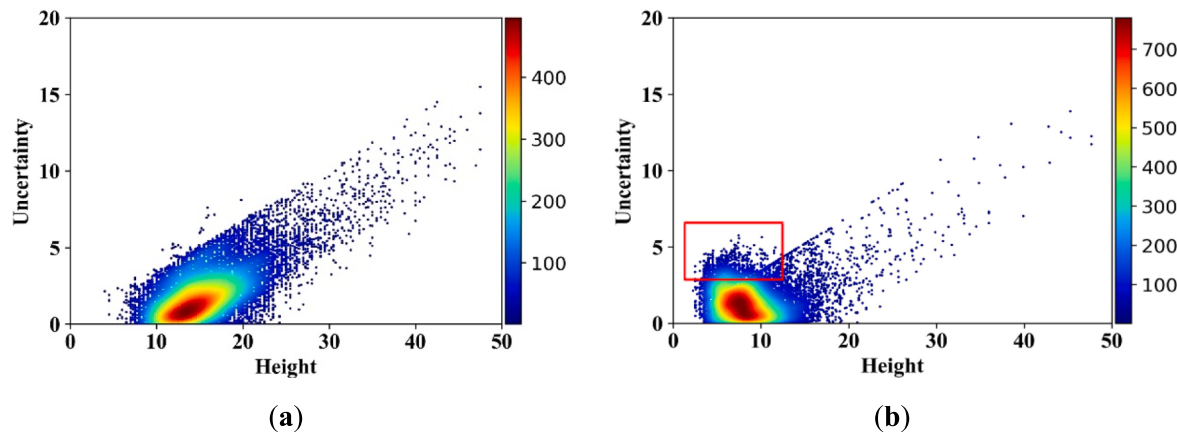


Fig. 7. RVoG height standard deviation and mean height in a two-dimensional histogram. The horizontal axis is the sampled forest height values and the vertical axis is the related uncertainties. (a) L-band; (b) P-band. The legends show the number of samples.

Table 3

Quantitative analysis of the uncertainty difference resulted from canopy type at L- and P-bands.

forest structure	band	Mean forest height value from LiDAR /m	Acc.	ratio of uncertainty
pure coniferous	L	15.22	0.90	0.09
canopy	P		0.63	0.15
pure broadleaf	L	12.48	0.63	0.13
canopy	P		0.78	0.09
mixed coniferous	L	11.73	0.74	0.16
canopy	P		0.61	0.27
mixed broadleaf	L	9.61	0.64	0.25
canopy	P		0.77	0.13
mixed coniferous and broadleaf canopy	L	11.21	0.55	0.21
	P		0.75	0.26

Table 4

Quantitative analysis of the uncertainty difference resulted from forest density at L and P bands.

Forest density (stems/ha)	Band	Mean forest height value from LiDAR /m	Acc.	Average absolute error	ratio of uncertainty
300–600	L	9.53	0.51	7.00	0.27
	P		0.66	0.62	0.24
600–1200	L	14.10	0.59	4.66	0.17
	P		0.77	1.31	0.23
1200–1800	L	12.34	0.79	2.45	0.13
	P		0.72	1.90	0.11

pure broadleaf canopy and mixed canopy types involved in broadleaf canopy.

Different canopy types correspond to different forest canopy structures, pure coniferous forest has more homogeneous canopy while pure broadleaf forest and mixed forest has more heterogeneous canopy. With the gradual increasing of the complexity of the forest canopy, P band showed higher prediction accuracy than the L band. When the forest canopy is simple like pure coniferous canopy or mixed coniferous canopy, the prediction accuracies at L band are high with Acc. values of 0.90 and 0.74 respectively. The accuracy values are higher than the prediction accuracies of P band with Acc. = 0.63 and Acc. = 0.61. When the forest canopy is more complex like pure broadleaf canopy or mixed broadleaf canopy, the prediction accuracies of the L band are 0.63 and 0.64 respectively, which are lower than the prediction accuracies of the P band. It seems that as the complexity of the forest canopy becomes

larger, the prediction accuracy of the L band gradually decreases, while the prediction accuracy of the P band gradually increases to a more stable level. The results may result from the different penetration capability of two bands, the lower penetration capability at L band make it difficult to distinguish the ground phase center with canopy scattering phase center, which resulted in the closer distance between two phase centers becomes more and more undistinguishable with the increasing of complex of forest canopy. The poor performance of P band in pure coniferous canopy may result from unsuitable RVoG model assumptions in these forests since the large value of ratio of effective ground-to-volume scattering and small extinction or its variation with the change of polarimetric, etc., which makes a mismatch between the observed coherence and the modeled coherence (Riel et al., 2018; Simard and Denbina, 2018).

The influences of canopy type on estimated forest parameter using remote sensing features were addressed in other studies (Jiang et al., 2020; Chowdhury et al., 2013; Gao et al., 2018; Zhao et al., 2016). However, most of them focused on inversion of forest AGB, meanwhile, their influence on estimation uncertainties were not fully and deeply explored. Zhang et al., (2023a) explored the effects of canopy type on uncertainties of estimated forest height through L band simulated PolInSAR data. The ratio of uncertainty was used in this study as well, the results demonstrated the uncertainty and the ratio of uncertainty for forest height estimation in coniferous canopy are lower than that in broadleaf canopy. Most of the $U(\bar{X})$ values for the pure coniferous canopy were around 0.10 while 0.20 for the pure broadleaf canopy in ideal situation. The results from it also confirmed worse performance of L band in mixed coniferous canopy than in pure coniferous canopy. For the difference performance and uncertainties acquired at L and P band, previous studies agree they maybe result from the different penetration capability at two bands which lead to the different suitability of two bands to the RVoG model (Simard and Denbina, 2018). The studies from previous study and this study confirmed that combining various input observations with Bayesian principles enables a reliable evaluation of a model's plausibility. (Beck and Yuen, 2004). Through the canopy type effect analysis at L and P band, we found L band suitable for forest height inversion with homogeneous canopy and P band for forest height inversion with heterogeneous canopy when RVoG model were used as the inversion vegetation scattering model.

From Table 4, we found that the ratio of uncertainty of the forest height inversion decreases with increasing of forest density. This may result from the fact that the μ is affected by the change in forest density. Since the ratio is a key model parameter in RVoG model and usually assumed as 0, it may result in great error in the sparse vegetation covered area (Wang et al., 2016).

In Table 4, When the forest density increased from 300 to 600 stems/

ha to 600–1200 stems/ha, the uncertainties at L and P band decreased 26 % and 17 %, respectively, indicating that L band was affected more by forest density than P band. Meanwhile, the absolute error can also characterize the influence of forest density on the results, when it increased from the 300–600 stems/ha to 1200–1800 stems/ha, the absolute error of the results estimated using L band decreased from 7.00 m to 2.45 m, while the largest difference for P band is only 1.58 m. When the forest density continued to increase to more than 1200 stems/ha, the uncertainty of the L band decreased by 21 % and the P band decreased by 13%. The prediction accuracy of the inversion outcomes also increased gradually with the rise in forest density, and the highest prediction accuracy was obtained by using the L band in forest stands larger than 1200 stems/ha, with a prediction accuracy of 0.79, while the prediction accuracy of the L band was as low as 0.51 in sparsely vegetated areas (300–600 stems/ha), which indicates that the L band PolInSAR data are not suitable for forest height inversion in sparsely vegetated areas with RVoG model. P band prediction accuracy and each uncertainty characterization are basically better than the L band, which may be attributed to the stronger penetration of P band. Better penetration capability made P band can better detect the information characterizing the ground. The results suggests that when the forest scenario is consistent with the model assumptions (e.g., the ratio between ground and volume scattering tends to zero as the forest density increases, or the data better characterize the ground phase information), the high prediction accuracy is accompanied by less uncertainty and the model shows good performance. Note that, according to the mean forest height acquired in different forest density, the values of the P band at different density level are all lower than that of the L band, which also verifies that the phases of the P band PolInSAR data are more concentrated in the complex plane, and that the ground scattering center will have a smaller difference from the volume scattering center (Xing et al., 2023; Riel et al., 2018). Previous study of uncertainties resulted from changes from forest densities using simulated forest scenes and L band PolInSAR dataset also confirmed the lower uncertainties in forest areas with high forest density (Zhang, et al., 2023a).

4. Conclusions

In this study, we explored the uncertainties of forest height estimated by RVoG model using a hierarchical Bayesian framework. The uncertainty differences resulted from the changes of microwave wavelength, canopy types, and forest density were analyzed detailly with values of uncertainty (standard derivation) and the ratio of uncertainty. The way we used here to calculated the uncertainties of inversion results is straightforward and robust. Canopy types had a clear impact on forest height estimate findings and the effects are different at L and P band. For pure coniferous canopy, lowest uncertainties were acquired at L band, while for pure broadleaf canopy or mixed forest involved in broadleaf canopy, low uncertainties acquired by P band. Forest density also has great effects on uncertainties of forest heights estimated by RVoG model. The high the forest density, the more stable of the estimated results with higher prediction accuracy and the lower of the uncertainties. However, in this study, with the limitation datasets and availability of detail prior knowledges of forest extinction at P band, other factors like length of baselines, the suitability of model assumption and their effects on the uncertainties of the forest heights estimated by RVoG model and PolInSAR datasets were not explored and deeply analyzed. In the future, the related studies need to further explored and analyzed.

CRediT authorship contribution statement

Han Zhao: Writing – original draft, Visualization, Validation, Software, Methodology, Formal analysis, Data curation. **Tingwei Zhang:** Visualization, Methodology, Formal analysis, Data curation, Conceptualization. **Yongjie Ji:** Supervision, Software, Resources, Project administration. **Wangfei Zhang:** Writing – review & editing,

Supervision, Resources, Investigation, Funding acquisition, Formal analysis, Conceptualization.

Declaration of competing interest

The authors declare that they have no known competing financial interests or personal relationships that could have appeared to influence the work reported in this paper.

Data availability

The authors do not have permission to share data.

Acknowledgments

The authors would like to thank the BioSAR Team for providing datasets and the funding support from the NSFC with grant of 32371869, 32160365, 42161059, and 31860240.

References

- Beck, J.L., Yuen, K.-V., 2004. Model selection using response measurements: Bayesian probabilistic approach. *J. Eng. Mech.* 130, 192–203.
- Chowdhury, T., Thiel, C., Schmullius, C., Stelmaszczuk-Górska, M., 2013. Polarimetric parameters for growing stock volume estimation using ALOS PALSAR L-band data over Siberian forests. *Remote Sens. (Basel)* 5, 5725–5756.
- Cloude, S., 2009. Polarisation: applications in remote sensing. OUP Oxford.
- Cloude, S.R., Papathanassiou, K.P., 1998. Polarimetric SAR Interferometry. *IEEE Trans. Geosci. Remote Sens.* 36.
- Cloude, S.R., Papathanassiou, K.P., 2003. Three-stage inversion process for polarimetric SAR interferometry. *IEEE Proc., Radar Sonar Navig.* 150, 125.
- Gao, Y., Lu, D., Li, G., Wang, G., Chen, Q., Liu, L., Li, D., 2018. Comparative analysis of modeling algorithms for forest aboveground biomass estimation in a subtropical region. *Remote Sens. (Basel)* 10, 627.
- Hajnsek, I., Kugler, F., Lee, S.-K., Papathanassiou, K.P., 2009. Tropical-forest-parameter estimation by means of Pol-InSAR: the INDREX-II campaign. *IEEE Trans. Geosci. Remote Sensing* 47, 481–493.
- Jiang, X., Li, G., Lu, D., Chen, E., Wei, X., 2020. Stratification-based forest aboveground biomass estimation in a subtropical region using airborne lidar data. *Remote Sens. (Basel)* 12, 1101.
- Krieger, G., Moreira, A., Fiedler, H., Hajnsek, I., Werner, M., Younis, M., Zink, M., 2007. TanDEM-X: a satellite formation for high-resolution SAR interferometry. *IEEE Trans. Geosci. Remote Sens.* 45, 3317–3341.
- Kugler, F., Lee, S.-K., Hajnsek, I., Papathanassiou, K.P., 2015. Forest height estimation by means of Pol-InSAR data inversion: the role of the vertical wavenumber. *IEEE Trans. Geosci. Remote Sens.* 53.
- Lang, N., Kalischek, N., Armstrong, J., Schindler, K., Dubayah, R., Wegner, J.D., 2022. Global canopy height regression and uncertainty estimation from GEDI LIDAR waveforms with deep ensembles. *Remote Sens. Environ.* 268, 112760.
- Lavalle, M., Khun, K., 2014. Three-baseline approach to forest tree height estimation, in: EUSAR 2014; 10th European Conference on Synthetic Aperture Radar, pp. 1–3.
- Lavalle, M., Hensley, S., 2015. Extraction of structural and dynamic properties of forests from polarimetric-interferometric SAR data affected by temporal decorrelation. *IEEE Trans. Geosci. Remote Sensing* 53, 4752–4767.
- Lavalle, M., Simard, M., Hensley, S., 2012. A temporal decorrelation model for polarimetric radar interferometers. *IEEE Trans. Geosci. Remote Sensing* 50, 2880–2888.
- Lee, S.-K., Kugler, F., Papathanassiou, K.P., Hajnsek, I., 2013. Quantification of temporal decorrelation effects at L-band for polarimetric SAR interferometry applications. *IEEE J. Sel. Top. Appl. Earth Observations Remote Sensing* 6, 1351–1367.
- Li, J., 2003. Error theory and measurement uncertainty evaluation. China Measuring Press, China.
- Li, W., Chen, E., Li, Z., Feng, Q., Yang, H., Li, X., 2015. Application performance analysis of spectral analysis techniques in forest vertical structure information extraction using tomographic SAR. *Acta Electron. Sinica* 43, 2646–2665.
- Liao, Z., He, B., Quan, X., 2020. Potential of texture from SAR tomographic images for forest aboveground biomass estimation. *Int. J. Appl. Earth Obs. Geoinf.* 88, 102049.
- López-Martínez, C., Alonso-González, A., 2013. Assessment and estimation of the RVoG model in polarimetric SAR interferometry. *IEEE Trans. Geosci. Remote Sens.* 52, 3091–3106.
- Neumann, M., Saatchi, S.S., Ulander, L.M.H., Fransson, J.E.S., 2012. Assessing performance of L- and P-band polarimetric interferometric SAR data in estimating boreal forest above-ground biomass. *IEEE Trans. Geosci. Remote Sensing* 50, 714–726.
- Ni, Y., 2014. Evaluation of practical measurement uncertainty. China Standard Press, China.
- Pang, S., Li, G., Jiang, X., Chen, Y., Lu, Y., Lu, D., 2022. Retrieval of forest canopy height in a mountainous region with ICESat-2 ATLAS. *Forest Ecosyst.* 9, 100046.
- Papathanassiou, K.P., Cloude, S.R., 2001. Single-baseline polarimetric SAR interferometry. *IEEE Trans. Geosci. Remote Sensing* 39, 2352–2363.

- Papathanassiou, K.P., Cloude, S.R., 2003. The effect of temporal decorrelation on the inversion of forest parameters from Pol-InSAR data. In: IGARSS 2003. 2003 IEEE International Geoscience and Remote Sensing Symposium. Proceedings (IEEE Cat. No.03ch37477). IEEE, Toulouse, France, pp. 1429–1431.
- Reigber, A., Moreira, A., 2000. First Demonstration of Airborne SAR Tomography Using Multibaseline L-Band Data. *IEEE Trans. Geosci. Remote Sens.* 38.
- Riel, B., Denbina, M., Lavalle, M., 2018. Uncertainties in forest canopy height estimation from polarimetric interferometric SAR data. *IEEE J. Sel. Top. Appl. Earth Observations Remote Sensing* 11, 3478–3491.
- Romero-Puig, N., Marino, A., Lopez-Sanchez, J.M., 2022. Application of the trace coherence to HH-VV PolInSAR TanDEM-X data for vegetation height estimation. *IEEE Trans. Geosci. Remote Sensing* 60, 1–10.
- Roueff, A., Arnaubec, A., Dubois-Fernandez, P.C., Refregier, P., 2011. Cramer-rao lower bound analysis of vegetation height estimation with random volume over ground model and polarimetric SAR interferometry. *IEEE Geosci. Remote Sensing Lett.* 8, 1115–1119.
- Simard, M., Denbina, M., 2018. An assessment of temporal decorrelation compensation methods for forest canopy height estimation using airborne L-band same-day repeat-pass polarimetric SAR interferometry. *IEEE J. Sel. Top. Appl. Earth Observations Remote Sensing* 11, 95–111.
- Soja, M.J., Sandberg, G., Ulander, L.M.H., 2013. Regression-based retrieval of boreal forest biomass in sloping terrain using P-band SAR backscatter intensity data. *IEEE Trans. Geosci. Remote Sensing* 51, 2646–2665.
- Tabb, M., Orrey, J., Flynn, T., Carande, R., 2002. Phase diversity: a decomposition for vegetation parameter estimation using polarimetric SAR interferometry. Proceedings of the European Conference on Synthetic Aperture Radar EUSAR, pp. 1–4.
- Tebaldini, S., d'Alessandro, M.M., Ulander, L.M.H., Bennet, P., Gustavsson, A., Coccia, A., Macedo, K., Disney, M., Wilkes, P., Spors, H.-J., Schumacher, N., Hanus, J., Novotný, J., Brede, B., Bartholomeus, H., Lau, A., Van Der Zee, J., Herold, M., Schuettemeyer, D., Scipal, K., 2023. TomoSense: A unique 3D dataset over temperate forest combining multi-frequency mono- and bi-static tomographic SAR with terrestrial, UAV and airborne lidar, and in-situ forest census. *Remote Sens. Environ.* 290, 113532.
- Wang, C., Wang, L., Fu, H., Xie, Q., Zhu, J., 2016. The impact of forest density on forest height inversion modeling from polarimetric InSAR data. *Remote Sens. (Basel)* 8, 291.
- Wu, C., Yang, X., Yu, Y., Tebaldini, S., Zhang, L., Liao, M., 2022. Assessment of underlying topography and forest height inversion based on TomoSAR methods. *Geo-Spatial Inform. Sci.* 1–16.
- Xiao, M., 1985. Error theory and application. China Measuring Press, China.
- Xing, C., Wang, H., Zhang, Z., Yin, J., Yang, J., 2023. A review of forest height inversion by PolInSAR: theory, advances, and perspectives. *Remote Sens. (Basel)* 15, 3781.
- Xu, K., Zhao, L., Chen, E., Li, K., Liu, D., Li, T., Li, Z., Fan, Y., 2022. Forest height estimation approach combining P-band and X-band interferometric SAR data. *Remote Sens. (Basel)* 14, 3070.
- Zhang, W., Chen, E., Li, Z., Zhao, L., Ji, Y., 2017. Development of forest height estimation using in-SAR/PolInSAR technology. *Remote Sens. Technol. Appl.* 32, 983–997.
- Zhang, T., Ji, Y., Zhang, W., 2022. The analysis on uncertainty resulting from method and wavelength selecting in forest height inversion using simulated polarimetric interferometric SAR data. *National Remote Sens. Bull.* 26, 1963–1975.
- Zhang, T., Zhang, W., Zhang, Y., Huang, G., 2023a. Bayesian analysis for uncertainty of forest height inversed by polarimetric interferometric SAR data. *National Remote Sens. Bull.* 27, 2431–2444.
- Zhang, Y., Zhao, H., Ji, Y., Zhang, T., Zhang, W., 2023b. Forest height inversion via RVoG model and its uncertainties analysis via Bayesian framework—comparisons of different wavelengths and baselines. *Forests* 14, 1408.
- Zhao, L., Chen, E., Li, Z., Zhang, W., Fan, Y., 2022. A new approach for forest height inversion using X-band single-pass InSAR coherence data. *IEEE Trans. Geosci. Remote Sensing* 60, 1–18.
- Zhao, P., Lu, D., Wang, G., Wu, C., Huang, Y., Yu, S., 2016. Examining spectral reflectance saturation in landsat imagery and corresponding solutions to improve forest aboveground biomass estimation. *Remote Sens. (Basel)* 8, 469.